OWNSHIP INTERFERENCE CANCELLATION AND SOURCE LOCALIZATION

Ivars P. Kirsteins[†], *José M. F. Moura*[‡], *John W. Fay*[†], *and Sanjay K. Mehta*[†]

[†]Naval Undersea Warfare Center
Newport Division
Code 3124, Code 3112
Newport, RI 02841 USA

[‡]Dep. Electrical and Computer Engineering
Carnegie Mellon University
5000 Forbes Ave.
Pittsburgh, PA 15213–3890 USA

ABSTRACT

Ownship radiated noise, direct and multipath, is a major source of interference that masks target signatures and makes them undetectable by classical techniques. It is especially a problem in the case of fast ship speeds and short tow cables in shallow water environments. In such cases, interference suppression techniques are needed to cancel this noise and unmask signals while maintaining a low false alarm rate. The paper shows that beamformers that account for the environmental conditions and suppress the interference provide substantial gains. Matching to the propagation conditions is particularly important. These gains become limited when the environment is progressively innacurately specified.

1. INTRODUCTION

Ownship radiated interference suppression is usually based on simple adaptive Wiener filters that do not exploit the physics of the propagation. These conventional LMS-based approaches have relatively long convergence times and hence have difficulty in suppressing highly nonstationary interference from ownship. This paper is a first attempt to understand the impact of a strong interference and of the media propagation effects on the performance of several beamformers. We present the output signal-to-noise ratio (SNR) among different beamformers operating in shallow water in the presence of interference. We study: the conventional beamformer $\mathrm{B_{conv}}$; the null-steering beamformer $\mathrm{B_{null}}$; a matched-field beamformer $\mathrm{B_{mfp}}$that is matched to the environmental propagation effects but ignores the presence of the interference; and the optimal minimum mean square error beamformer $\mathrm{B_{opt}}$ (Wiener beamformer) that accounts for the interference cancellation and is matched to the propagation environment. A fifth beamformer, the whitening beamformer $\mathrm{B_{white}}$, was also tested, but, for strong interference, the results parallel those of $\mathrm{B_{null}}$, so it is not considered explicitly here. We also illustrate the sensitivity of the beamformers to lack of complete knowledge of the environment.

Our conclusions are interesting. They show that, by accounting for propagation physics explicitly, significantly improved interference suppression and detection is attained. Further, accounting for the environment (matched-field-processing) has a larger performance impact than nulling the interference. On the other hand these gains provided by the $\mathrm{B_{opt}}$ and the $\mathrm{B_{mfp}}$ are significantly reduced when there are small mismatches in the assumed target or interferer ranges, or in the sound velocity.

In section 2, we describe the interference problem geometry. In section 3, we consider shallow water propagation models. In section 4, we present the beamformers of interest in our study and the figures-of-merit to be used. Finally section 5 studies the performance of the beamformers of section 4 and their sensitivity to lack of complete knowledge of the environment.

2. PROBLEM

Figure 1 depicts the geometry of interest. The water channel is shallow with depth h. A horizontal linear array of K hydrophones at depth d_a is towed by a surface ship. Propeller, cavitation, and other noise sources of the towing ship are illustrated as a pointwise single tone interference noise source located at depth d_i and range R_0 (distance to the leftmost hydrophone). A noisy source at depth d_s, range R (distance to the leftmost hydrophone), and bearing angle θ (measured with respect to broadside) radiates also a pure tone. The interference tone frequency f_{int} and the source tone frequency f_s will be taken to be equal. We define the angular frequency $\omega = 2\pi f$. The array intersensor spacing is $\delta = \lambda/2$ with the wavelength $\lambda = c/f$, where c is the medium sound velocity.

0-7803-5045-6/98/$10.00 ©1998 IEEE

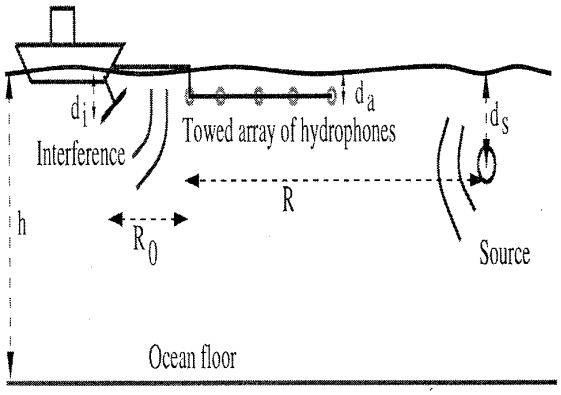

Figure 1: Problem geometry

3. SHALLOW WATER: NORMAL MODES

Initially, we assume that the water channel is a homogeneous single layer (the environment is range independent and isovelocity), with a perfectly rigid bottom and ideal pressure release surface. We work with the harmonic solution to the wave equation (single frequency). Using normal modes and with the far-field approximation, i.e., at large distances from the source as compared to the wavelength (so that a Hankel function can be well approximated by the first term of its asymptotic representation), the potential function (acoustic field pressure), suitably normalized, is given by [1, 2]

$$p(r, z_s, z_r, t) \propto \exp(-j\omega t) \tag{1}$$

$$\sum_{l=0}^{\infty} \frac{1}{\sqrt{\xi_l r}} \sin(\alpha_l z_s) \sin(\alpha_l z_r) \exp[j(\xi_l r - \pi/4)]$$

$$\begin{aligned} \xi_l &= \pm[k^2 - (\pi/h)^2(l+1/2)^2]^{1/2}, \quad l = 0, 1, \cdots \\ \alpha_l &= (\pi/h)(l+1/2) \qquad\qquad l = 0, 1, \cdots \end{aligned}$$

where r, z_s ($=d_s$ or d_i), and z_r ($=d_a$) are the range, source depth, and receiver depth variables, and $k = 2\pi/\lambda = \omega/c$ is the wavenumber. Depending on whether $(\pi/kh)(l+1/2)$ is less than or greater than unity, the normal mode will propagate without attenuation or decrease exponentially with distance, respectively, [1, 2].

For more realistic shallow water environments, we will apply the normal mode model KRAKEN [3, 4]. In particular we use the code developed in [5].

4. BEAMFORMERS

The signal received at the K elements of the array, after quadrature demodulation, is the K-dimensional vector

$$\mathbf{y} = \beta_s \mathbf{S} + \beta_{\text{int}} \mathbf{X} + \mathbf{n}$$

where $\mathbf{S}$ is the transmitted source signal and $\mathbf{X}$ is the interference signal, both at the array sensors. The noise $\mathbf{n}$ is additive zero mean white Gauss with normalized unit variance. The variables β_s and β_{int} are independent Gauss random variables with zero mean and variances σ_s^2 and σ_{int}^2, respectively.

The signals $\mathbf{S}$ and $\mathbf{X}$ are given by the mode expansion in equation (1) representing the complex propagation structure in shallow water, or computed with KRAKEN, and are normalized to unit power in the following way. If, for example, $\widetilde{\mathbf{S}}$ is the received (vector) source signal at the array as computed from equation (1) after propagation in the shallow water channel, then we normalize $\mathbf{S}$ in the following way

$$S_{\text{power}} = \frac{1}{K} \sum_{k=1}^{K} |\widetilde{\mathbf{S}}_k|^2 \tag{2}$$

$$\mathbf{S} = \widetilde{\mathbf{S}} / \sqrt{S_{\text{power}}}, \tag{3}$$

and likewise for $\mathbf{X}$.

We define the (planar wavefront) steering vector $\mathbf{S_b}$

$$\widetilde{\mathbf{S_b}} = [1 \gamma \gamma^2 \cdots \gamma^{K-1}]^H \tag{4}$$

$$\mathbf{S_b} = \widetilde{\mathbf{S_b}} / \sqrt{\widetilde{S_b}}$$

where $\gamma = \exp\{-j2\pi f_{\text{int}} \Delta\}$, $\Delta = (\delta/c)\sin\theta$, θ is the bearing angle (with respect to broadside), and $\widetilde{S_b}$ is the power of $\widetilde{\mathbf{S_b}}$ defined similarly to equation (2).

We introduce the covariance $\mathbf{N}$ of the interference plus noise term

$$\mathbf{N} = \sigma_{\text{int}}^2 \mathbf{X}\mathbf{X}^H + \mathbf{I}. \tag{5}$$

We consider the output signal-to-noise ratio (SNR) for the following beamformers.

Conventional Beamformer $\mathbf{B}_{\text{conv}}$ This is the conventional beamformer. It ignores the presence of the interference and the propagation environment. It reduces to a simple DFT of the outputs of the array sensors. The output SNR is defined as

$$\text{SNR}_{\text{conv}} = \frac{|\sqrt{\sigma_s^2}\, \mathbf{S_b}^H \mathbf{S}|^2}{\mathbf{S_b}^H \mathbf{N} \mathbf{S_b}}$$

Null Steering Beamformer $\mathbf{B}_{\text{null}}$ This beamformer places a null at the direction of the interference, but ignores the complex environment propagation conditions. It uses the steering vector in equation (4) rather than the generalized steering vectors matched to the shallow water propagation conditions. It assumes perfect knowledge of the interference and signal time and statistical characteristics. The null-steerer filter weights

are $\mathbf{w}_{\text{null}} = \left(\mathbf{I} - \frac{\mathbf{X}\mathbf{X}^H}{||\mathbf{X}||_F}\right)\mathbf{S_b}$ and the output SNR is

$$\text{SNR}_{\text{null}} = \frac{|\sqrt{\sigma_s^2}\mathbf{w}_{\text{null}}^H\mathbf{S}|^2}{\mathbf{w}_{\text{null}}^H\mathbf{w}_{\text{null}}}$$

The whitening beamformer B_{white} 'whitens' the observations using the 'interference + noise' covariance given in equation (5). The weights are $\mathbf{w}_{\text{white}} = \mathbf{N}^{-1}\mathbf{S_b}$. However, for strong interferences, the case of interest here, the output SNR is indistinguishable for both B_{null} and B_{white}, so we don't consider B_{white} further.

Matched Field Beamformer $\mathbf{B}_{\text{mfp}}$ This beamformer ignores the interference. It uses the generalized steering vectors matched to the shallow water acoustics propagation. These generalized steering vectors $\mathbf{S}$ are determined using knowledge of the relative source/ array position and the assumed propagation model, given either by equations (1) and (3), or by the KRAKEN model [3, 4, 5]. It assumes perfect knowledge of the source location and of the environment. The output SNR is

$$\text{SNR}_{\text{mfp}} = \frac{|\sqrt{\sigma_s^2}\mathbf{S}^H\mathbf{S}|^2}{\mathbf{S}^H\mathbf{N}\mathbf{S}}$$

Optimal Beamformer $\mathbf{B}_{\text{opt}}$ This beamformer combines the nulling of the interference with the propagation models for shallow water. It assumes perfect knowledge of the interference and source location as well as the environment. The output SNR is

$$\text{SNR}_{\text{opt}} = \sigma_s^2\,\mathbf{S}^H\mathbf{N}^{-1}\mathbf{S}$$

Comments Comparing these beamformers enables the understanding of the relative role played by the environment and the interference. The optimal beamformer B_{opt} provides an upper bound on the performance to be expected. In contrast, the conventional beamformer B_{conv}, ignoring both the interference and environment, should represent a lower bound on the performance. The performance of the null steering beamformer B_{null} provides an indication of how much of the available gain between B_{conv} and B_{opt} can be attributed to the nulling of the interference, while the study of the B_{mfp} illustrates the gain that can be attributed to compensating for the propagation effects.

In the next section, we illustrate these gains for a variety of conditions. We also study the sensitivity of these gains to mismatches between the assumed and the actual environmental conditions.

5. PERFORMANCE RESULTS

The following values for the parameters in figure 1 and in section 2 determine the canonical configuration for our experiments: tone frequencies $f_s = f_{\text{int}} = 75$Hz; water depth $h = 130$m; interferer depth $d_i = 5$m; array tow depth $d_a = 30$m; signal source depth $d_s = 60$m; interferer true range to first hydrophone $R_0 = 350$m; array length $L = 350$m; sound velocity $c = 1500$m/s; intersensor spacing $\delta = \lambda/2$; source true range to first hydrophone $R = 10^4$m; source SNR=0 dB; interference to white noise ratio (INR)=10 dB. From SNR and INR we compute σ_s^2 and σ_{int}^2, respectively. Changes to this canonical configuration will be indicated on the body of the plots. We plot the SNR loss for the four beamformers of section 4 as a function of the source bearing angle $\theta \in [-\pi/2, \pi/2]$.

In each of the figures in this and the next section there are four plots: the dashed line (blue in color plots) (top line) corresponds to the B_{opt}; the solid line (black) (usually second top line) is for the B_{mfp}; the 'X' (magenta) is the B_{null}; and the dashdot line (red) is the B_{conv}.

Figure 2 plots the gains of the four beamformers for an isovelocity channel, where the field is computed with equation 1. Figure 3 is similar to figure 2, except

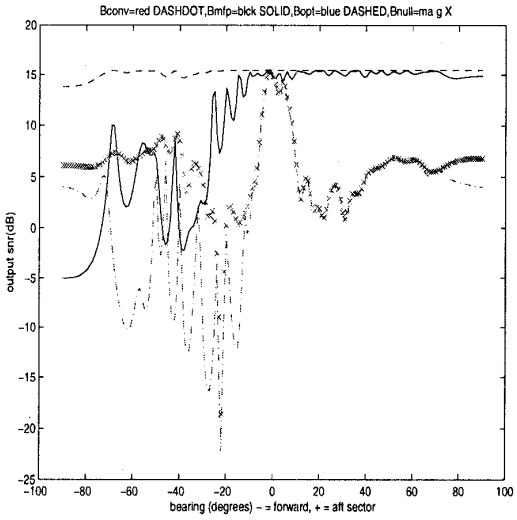

Figure 2: Shallower isovelocity channel, $f_s = f_{\text{int}} = 75$ Hz, $d_i = 5$m, $d_a = 30$m, $d_s = 60$m, $R_0 = 350$m, $R = 10^4$m, $h = 130$m

that it is for a deeper channel, and the interference, the array, and the source are at larger depths, with the interference further away from the array. These two plots basically illustrate a similar behavior for the beamformers. The B_{mfp} is remarkably better than the B_{null} and the B_{conv} for sources with bearings in $[-30°, 90°]$, i.e., from broadside to endfire away from the interference. Surprisingly, the B_{null} is not much better than B_{conv}, and their performance is only acceptable at broadside.

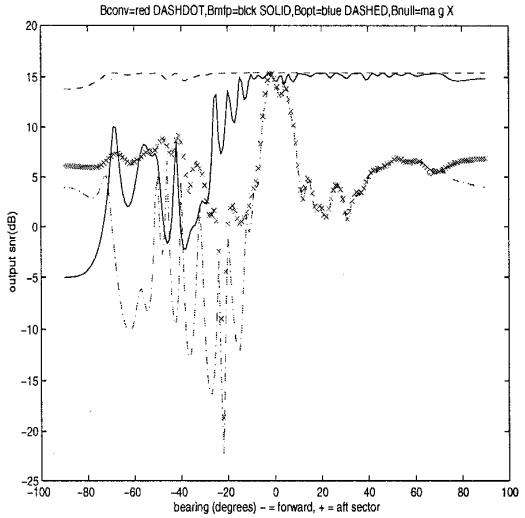

Figure 3: Deeper isovelocity channel; dashed: B_{opt}; solid B_{mfp}; dashdot B_{conv}; 'X' B_{null}

The top plot in figure 4 compares the performance of the beamformers for a KRAKEN run for conditions modeling the Straits of Malta in the Mediterranean Sea. The sound velocity profile is in the bottom plot in figure 4. For deeper interferer, array, and source (d_i = 10 m, d_a = 75 m, d_s = 100 m) similar performance was observed. The figure shows that all beamformers experience a noticeable loss of performance. The B_{mfp} performance improves as the source gets away from the interference in the bearing domain. Figure 5 shows the improvement that results with longer arrays (100 element array, L = 1000 m).

Performance under Mismatch Figures 6, 7, and 8 consider several degrees of mismatch. Figure 6 only assumes an error in the position of the interferer, figure 7 assumes in addition a mismatch in the source range, and finally figure 8 adds an error in the sound speed. As the degree of mismatch increases the performance of the B_{mfp} increasingly degrades. These figures reinforce the notion that matching to the environment seems to lead to a larger payoff than nulling the interference.

Acknowledgment The work of NUWC was sponsored by ONR Mechanics and Energy Conversion S&T Division. The work of CMU was partially supported by ONR grant N00014-97-1-0040 and Darpa through AFOSR grant F49620-96-1-0436.

6. REFERENCES

[1] L. M. Brekhovskikh and Y. P. Lysanov, *Fundamentals of Ocean Acoustics*. New York: Springer-Verlag, second edition ed., 1991.

[2] P. C. Etter, *Underwater Acoustic Modeling: Principles, Techniques and Applications*. New York: Elsevier Applied Science, 1991.

[3] M. B. Porter and E. L. Reiss, "A numerical method fort bottom interacting ocean acoustic normal modes," *Journal of the Acoustical Society of America*, vol. 77, pp. 1760–17767, 1985.

[4] M. B. Porter, "The KRAKEN normal mode program," Tech. Report Memorandum SM-245, Saclant Center, La Spezia, Italy, 1991.

[5] J. Ianniello, "A MATLAB version of the KRAKEN normal mode code," Tech. Report TM No. 94-1096, NUWC, New London, CT, October 1994.

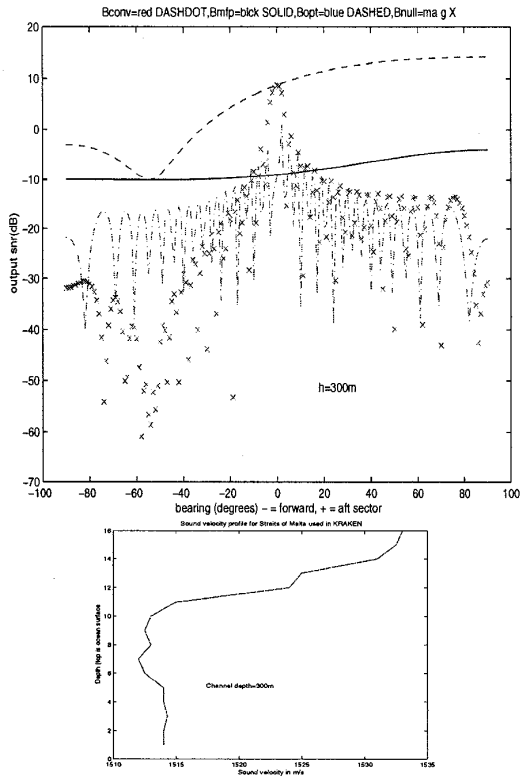

Figure 4: Straits of Malta: KRAKEN channel, $f_s = f_{int}$ = 75 Hz, d_i = 5m, d_a = 30m, d_s = 60m; R_0 = 350m, $R = 10^4$m. Top: Performance; bottom: sound velocity profile

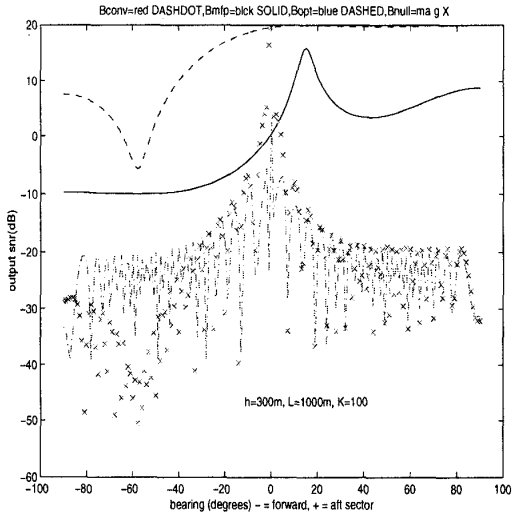

Figure 5: Straits of Malta: KRAKEN channel, long array; dashed: B_{opt}; solid B_{mfp}; dashdot B_{conv}; 'X' B_{null}

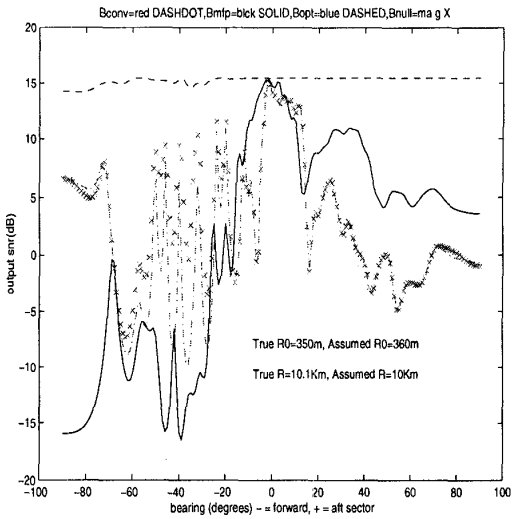

Figure 7: Isovelocity channel: Mismatch in R_0 and R

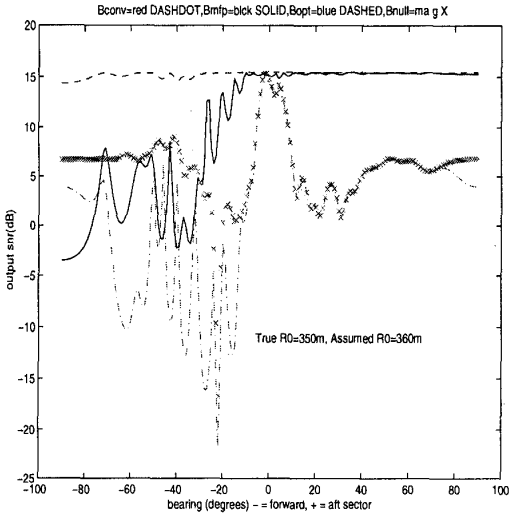

Figure 6: Isovelocity channel: Mismatch in $R0$, $f_s = f_{\text{int}} = 75$ Hz, $d_i = 5\text{m}, d_a = 30\text{m}, d_s = 60\text{m}, R_0 = 350\text{m}, R = 10^4\text{m}$

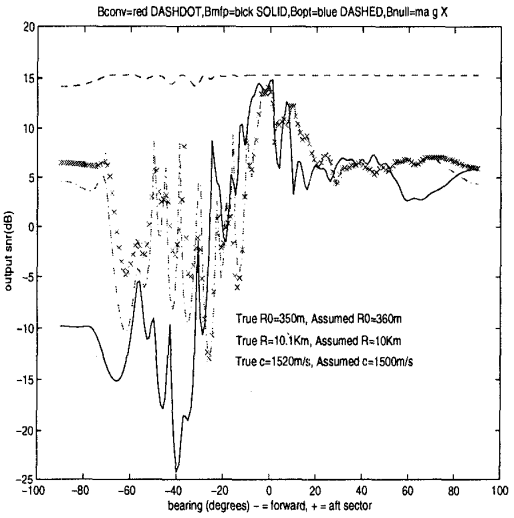

Figure 8: Isovelocity channel: Mismatch in R_0, R, c; dashed: B_{opt}; solid B_{mfp}; dashdot B_{conv}; 'X' B_{null}